

# Modelling of the limiting current density of an electro dialysis process by response surface methodology

Mourad Ben Sik Ali<sup>1,2</sup> · Amine Mnif<sup>2</sup> · Béchir Hamrouni<sup>2</sup>

Received: 7 April 2017 / Revised: 19 June 2017 / Accepted: 24 June 2017 / Published online: 17 July 2017  
© Springer-Verlag GmbH Germany 2017

**Abstract** Electrodialysis is an electro-membrane process for desalination, concentration, and separation in electric fields. In this process, the operating currents are limited by the concentration polarization phenomena and the limiting current density. Usually, this parameter depends on membrane and solution properties as well as on the electro dialysis stack construction. In this research paper, we will apply the Box–Behnken design in combination with response surface methodology to the development of a predictive limiting current density model. We will also study the effects of three variables related to solution composition (calcium, sulfate, and bicarbonate concentrations) on this parameter.

**Keywords** Electrodialysis · Limiting current density · Solution composition · Response surface methodology · Box–Behnken design

## Introduction

Electrodialysis (ED) and the related technologies are electro-chemical membrane separation processes in which ions are transferred through selective ion exchange membranes from one solution to another using an electric field as the driving force [1–4].

There has been a worldwide increase in the interest in the use of electro dialysis in the desalination process as well as in the removal of the excess inorganic contaminants such as borate, fluoride, and heavy metals from water [5–7]. This is mainly because of the increase in technology performances following the development of new membranes and new sources of energy. This technique ensures less defects than what chemical processes do [2, 3, 5].

In electro dialysis, it is desirable to work at relatively high current density in order to achieve fast desalination with the lowest possible effective membrane area [8]. In practice, however, concentration polarization phenomena restrict the operating currents [9–11]. Concentration polarization has been studied using a commercial anion and cation exchange membranes. The current voltage curves have showed the occurrence of a limiting current density (LCD). The limiting current density in the electro dialysis process is an important parameter which determines the electrical resistance and the current utilization. Usually, LCD depends on membrane and solution properties as well as on the electro dialysis stack construction and various operational parameters such as the flow velocity of the dilute solution [8, 11]. Therefore, a reliable determination of LCD is required for designing an efficient electro dialysis plant.

In a literature review, researchers have proposed many empirical expressions in which  $i_{lim}$  (LCD) is a function of the feed flow velocity in the stack ( $u$ ) and the concentration of dilute solution ( $C$ ). For example, Tanaka has proposed the following expression:

$$i_{lim} = m \times C^n \quad (1)$$

With  $m = 66.36 + 14.72 \times u$  and  $n = 0.7404 + 3.585 \times 10^{-3} \times u$ .

✉ Mourad Ben Sik Ali  
mourad.bensikali@gmail.com

<sup>1</sup> Engineering Preparatory Institute of Nabeul, Merezka University Campus, Merazka, 8000 Nabeul, Tunisia

<sup>2</sup> Desalination and Water Treatment Research Unit, Chemistry Department, Faculty of Sciences of Tunis, University of Tunis El Manar, 2092 Tunis, Tunisia

In his investigation, Tanaka used NaCl solutions and an electro dialysis unit incorporated with an Aciplex A172 anion exchange membrane [12–14].

Lee and Strathmann have also proposed an empirically derived expression in which  $i_{lim}$  is a function of the feed flow velocity in the stack and the concentration of dilute solution. The correspondent equation, which refers to Lee-Strathmann model, is:

$$i_{lim} = a \times C \times u^b \quad (2)$$

Where the coefficients  $a$  and  $b$  are constant;  $a$  is expressed in  $A s^b m^{1-b} keq^{-1}$  and  $b$  is dimensionless.

These coefficients ( $a$ ,  $b$ ,  $m$ , and  $n$ ) are estimated by the respective  $i_{lim}$  measurements with different flow velocities and different dilute concentration for a specific cell design.

Recently, Nakayama et al. have confirmed these results. In fact, they have found that the limiting current density is almost proportional to the feed velocity, since the proposed equation for the dialyser case with porous media suggests  $i_{lim} \propto u_d$  for substantial mechanical dispersion. Thus, for the dialyser case with porous media, the ion depletion on the membrane is retarded remarkably by increasing the feed velocity  $u_d$ . They have also stated that the spacer presence works to delay the possible depletion of the ions on the membrane dilute side, thus the limiting current density increases [15].

As shown, researchers have mainly focused on the effects of two parameters: the feed flow velocity in the stack as well as the feed solution concentration. However, we think that no studies have been conducted to study the effects of the feed solution composition on the value of the limiting current density.

Although it is not possible to establish an accurate model for the limiting current density, there are still some systematic methodologies for the determination and or the prediction of its value during electro dialysis processes. Response surface methodology (RSM) is such one method. RSM is an effective technique for analyzing the interactions among factors, exploring the relationships between the response and the independent variables, and optimizing the processes or products where multiple variables may influence the outputs [7, 16–20, 47].

The main advantage of RSM is the small number of experimental trials needed to evaluate multiple parameters and their interactions [16–18, 21, 22], and this makes the optimization process more efficient and cost-effective in terms of both manpower and resources.

In this study, Box–Behnken design (BBD) has been used for experimental design and data analysis. Box–Behnken designs are incomplete three-level factorial designs. They are built combining two-level factorial designs with incomplete block designs in a particular way. Box–Behnken designs have been introduced in order to limit the sample size as the number

of parameters grows. The sample size is kept to a value which is sufficient to estimate the coefficients in a second degree least squares approximating polynomial [46].

BBD has the advantage of requiring fewer experiments than would a full factorial design. Another advantage of the BBD is that it does not contain combinations for which all factors are simultaneously at their highest or lowest levels. So, these designs are useful in avoiding experiments performed under extreme conditions, for which unsatisfactory results might occur [23–25]. BBD has been widely utilized along with RSM to optimize various physical, chemical, and biological processes [26].

In this work, the influences of three independent variables calcium, sulfate, and bicarbonate concentrations of treated solution on the LCD were studied. These factors have been chosen because most brackish waters contain these ions at different amounts. On the other hand, our previous work showed that the desalination and purification processes of a brackish waters are closely influenced by these compounds [27, 48].

## Background

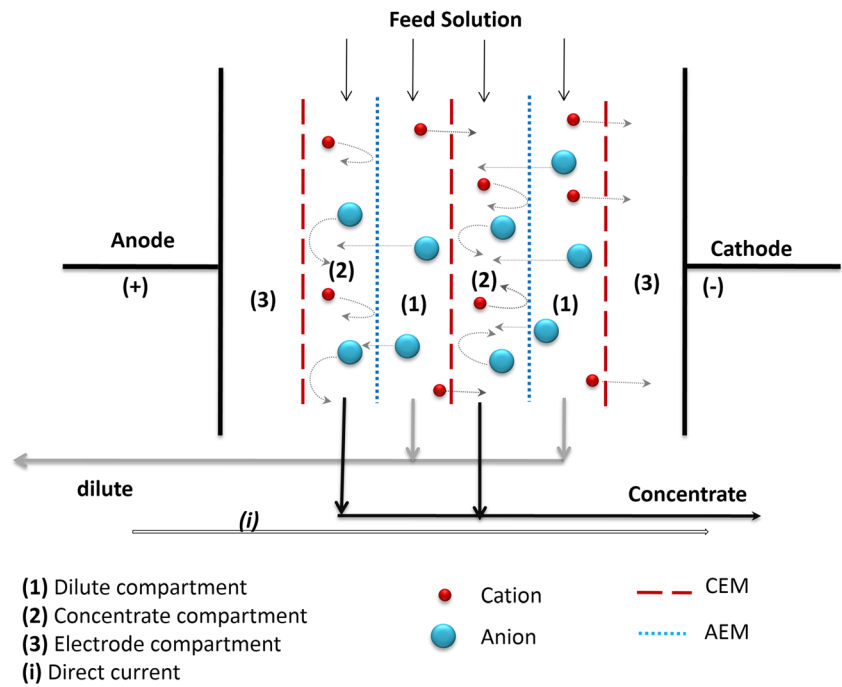
Electro dialysis is a separation process that is based on the selective migration of ions in solution through ion exchange membranes under the activation of an electric field [4, 28–30]. This process is widely used especially for brackish water desalination and sodium chloride recovery from seawater [1, 31–34].

As shown in Fig. 1, an ED system consists of a series of anion (anion exchange membrane (AEM), anion permeable) and cation exchange membranes (CEM, cation permeable) arranged in a parallel and alternate ways between two electrodes. While solutions are circulating through membranes, an electrical potential difference is applied between the two electrodes in the process. In response to the presence of the electric field, the ionized dissolved species contained in solutions such as salts, acids, or bases are selectively transported across the ion exchange membrane. Cations migrate toward the cathode, whereas anions gravitate to the anode target. However, the interposed CEM blocks the anions and allows the cations passage only while AEM blocks the cations and allows the anion migration.

Over time, one of the compartments is stripped of ions (diluted), while the other becomes more ionically populated (concentrated). Consequently, two different compartments emerge: concentrate compartment (concentrate) and dilute compartment (dilute).

In electro dialysis, as shown in Fig. 2, concentration polarization can take place at the membrane surface. An electric potential difference is obtained as a response to the application of current. This is the result of the speed at which the ions are

**Fig. 1** Principle of electro dialysis

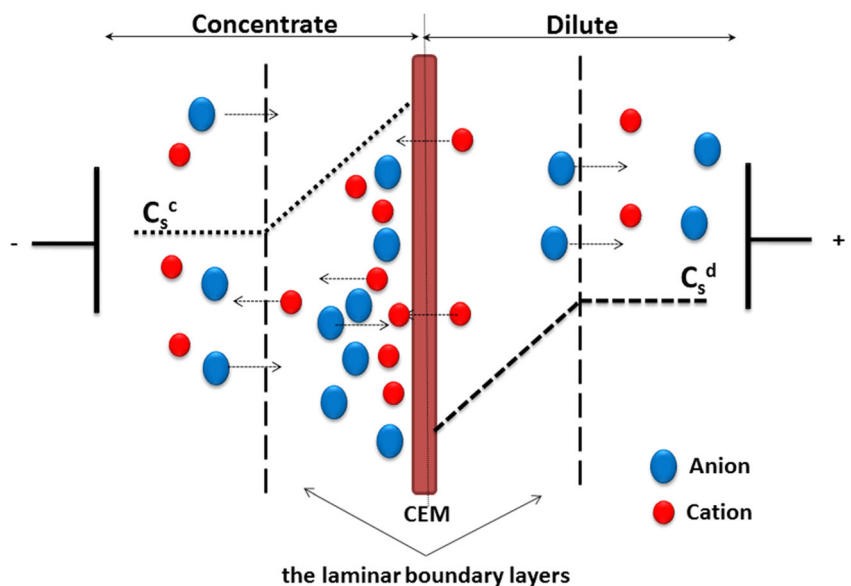


transported within the system. By increasing the potential difference, the current is also amplified as a result of the enhancement of the transport velocity of the ions that contact the membrane and then traverse it. However, since the rates of ion transport within the membrane and into the solution are different, this increase in the current attains a threshold where the ion concentration at the membrane/solution interface in the dilute cell ( $C_s^d$ ) is degraded to the point that any subsequent increase in the electric field results in the dissociation of water. In the other side, the charged species transport increases at the surface facing the concentrate cell ( $C_s^c$ ). When the ion concentration at membrane surface approaches the zero, the current density approaches the maximum value. At this

condition, the applied current is defined as the limiting current ( $i_{lim}$ ) and its density is called the LCD.

Beyond this point, an increase in cell resistance occurs and the pH of the solution is altered. This is mainly due to the quantity of charged species present at the membrane/solution interface. In fact, the population of ions in this area is not enough to carry an appropriate current flow. Hence, the  $H^+$  ions and  $OH^-$  products generated from the dissociation of water begin to conduct electrical current [29, 35]. This can cause a decrease in the efficiency system via the requirement for higher energy consumption. Also, the pH changes may lead to the precipitation of insoluble hydroxides on the membrane surface.

**Fig. 2** Schematic diagram of concentration polarization in electro dialysis process



The appearance of the concentration polarization phenomenon prevents the treatment of very dilute solutions in ED systems. Hence, it is convenient to operate the system at 80% of  $i_{lim}$  in order to harness the full extent of energy via ions transport.

To conclude, the limiting current density can be considered as one of the most important parameters in the electro dialysis process. It is, therefore, necessary to determine its value in order to prevent the problems and to operate the electro dialyzer effectively [8, 35, 36].

The concentration polarization magnitude is a function of various parameters including the applied current density, the feed flow velocity parallel to the membrane surface, the cell design, and the membrane properties [11, 12, 36, 37, 38, 49]. For a designed electro dialysis cell and for a treated solution at the same hydrodynamic conditions, the effects of the cell design and membranes characteristics on limiting current density can be considered as constant and can be neglected.

## Experimental

### Membranes and reagents

Ion exchange membranes were made at FuMA-Tech Company (Germany). The membrane types fumasep FKS and FAA are ion exchange homogeneous standard membranes with high chemical stability and good selectivity and conductivity. These membranes are intended to be used in standard demineralization applications in electro dialysis. Their corresponding properties are listed in Table 1.

Analytical grade sodium chloride (NaCl), calcium chloride (CaCl<sub>2</sub>), sodium bicarbonate (NaHCO<sub>3</sub>), and sodium sulfate (Na<sub>2</sub>SO<sub>4</sub>) salts are used in all experiments.

Synthetic brackish water solutions with known amount of compounds were prepared by dissolving these reagents in distilled water. Our previous work has shown that it is better not to increase the ionic strength of initial feed solution above 0.05 M since an electrode overheating can appear in the ED system as a

result of the increase in cell conductivity. Also, the desalination rate is very low and insignificant. For these reasons, it is suitable to use the ED process for the treatment of solution with salinity under 0.05 M [31]. Ionic strength was fixed (0.05 M) by adjusting the sodium chloride concentration. Since prepared solutions can contain bicarbonate ions, pH was adjusted to 7 (pH of neutral water) prior the start of the experiments by adding hydrogen chloride (HCl) and/or sodium Hydroxide (NaOH).

Sodium sulfate salt and distilled water have been used to prepare electrode rinse solution.

### Experimental installation

A FuMA-Tech® Lab scale Module “EDFT-ED-40” for electro-membrane processes was used in this work. It consists of two-cell pairs (two FAA and three FKS membranes) stacked between two titanium electrodes with a platinum layer.

As shown in Fig. 3, commercial spacers (FuMA-Tech) are placed between the membranes to form the flow paths of the dilute and concentrate streams.

These spacers are made of woven PVC/PET filaments. Each filament has a 0.2-mm diameter and forms a 90° angle when crossing another filament. Every two parallel filaments are distant of 1.1 mm from one another.

These spacers are designed to minimize boundary layer effects and are arranged in the stack so that all the dilute and concentrate streams are manifolded separately.

For each membrane, the active surface area is 0.0036 m<sup>2</sup> (90 mm × 40 mm) and the flow channel width between two membranes is 0.5 mm.

A direct current generator AL 924A (elc Company, France) was then connected to ED stack electrodes to assure an applied current between them. The brine, feed, and electrode rinse solutions were circulated in the unit using three centrifugal pumps equipped each with a flowmeter and three valves so as to control their flow rates.

Figure 4 shows a simplified diagram of the electro dialysis setup working in continuous mode. In this mode, the solutions pass only once in the cell. This type of operation is also called “single pass process.”

### Experimental procedure: determination of the limiting current

As reported in the literature, the limiting current ( $i_{lim}$ ) and then the LCD can be determined experimentally by plotting the electrical resistance across the membrane stack ( $E i^{-1}$ ) or the pH value in the dilute cell as a function of the reciprocal electric current ( $i^{-1}$ ). At the inflection point on this graph, the current intensity divided by the membrane area is

**Table 1** Information on ion exchange membranes

	Cation exchange membrane	Anion exchange membrane
Membrane	Fumasep FKS	Fumasep FAA
Thickness (mm)	0.11–0.13	0.13–0.15
Electric resistance ( $\Omega \text{ cm}^{-1}$ )	<8	2–4
Selectivity (%)	>96	>92
Swelling (%)	12–15	25
Ion exchange capacity ( $\text{meq g}^{-1}$ )	1.0	1.2

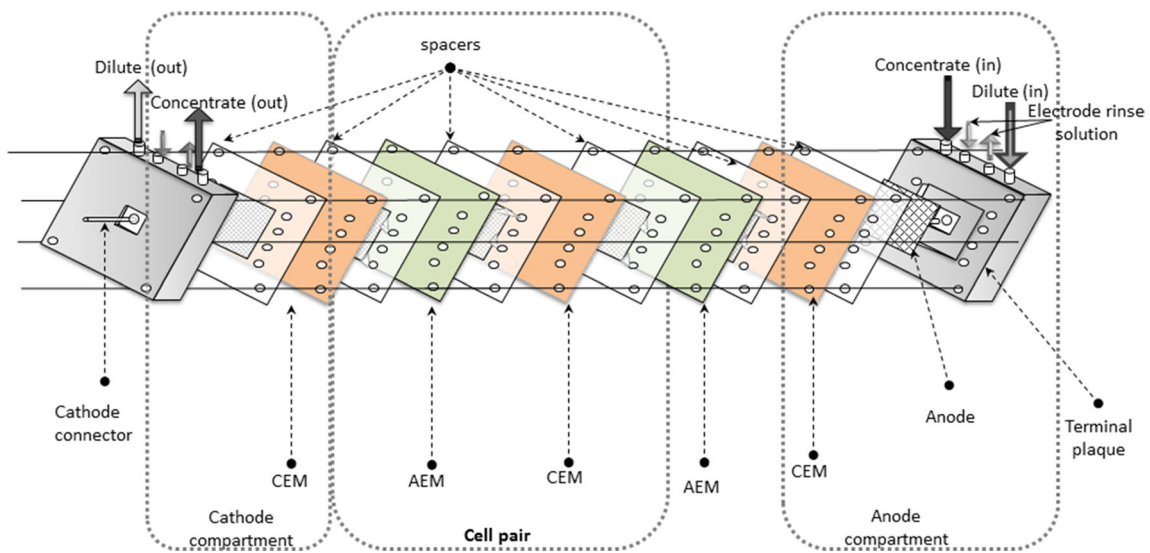


**Fig. 3** Schematic of the ED cell used in this study

considered as the  $i_{lim}$  value of the system. This is called a Cowan–Brown plot after its original developers [32, 36]. Figure 5 depicts two typical types of curves for the experimental determination of  $i_{lim}$  by the Cowan–Brown method.

In order to prevent the generation of chlorine or hypochlorite, which could be hazardous to the electrodes, 0.1 M  $\text{Na}_2\text{SO}_4$  has been used as electrode rinse solution circulating in electrode compartments. Flow rate of electrode rinse solution has been adjusted to  $80 \text{ L h}^{-1}$  for all experiments.

During the experiments, the same synthetic brackish water solutions have been used as initial concentrate and dilute solutions. Their flow rates (dilute and concentrate) have been adjusted to  $7 \text{ L h}^{-1}$  at the beginning of the experiment. Voltage between electrodes ( $E$ ) has also been fixed at the startup of the experiment using the direct current generator. The resulting electric current ( $i$ ) has then been determined by simple lecture from the same generator.

Samples have been collected at the inlet (before treatment) and outlet (after treatment) of each compartment of electro dialysis cell. The pH of each sample has then

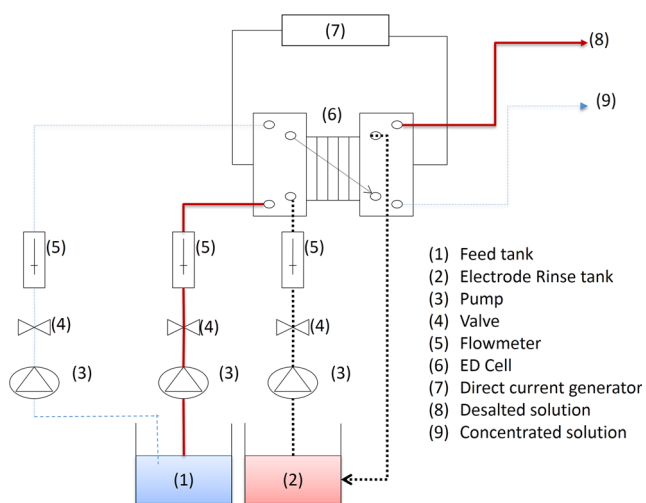


**Fig. 4** Schematic of the electro dialysis system used in this study

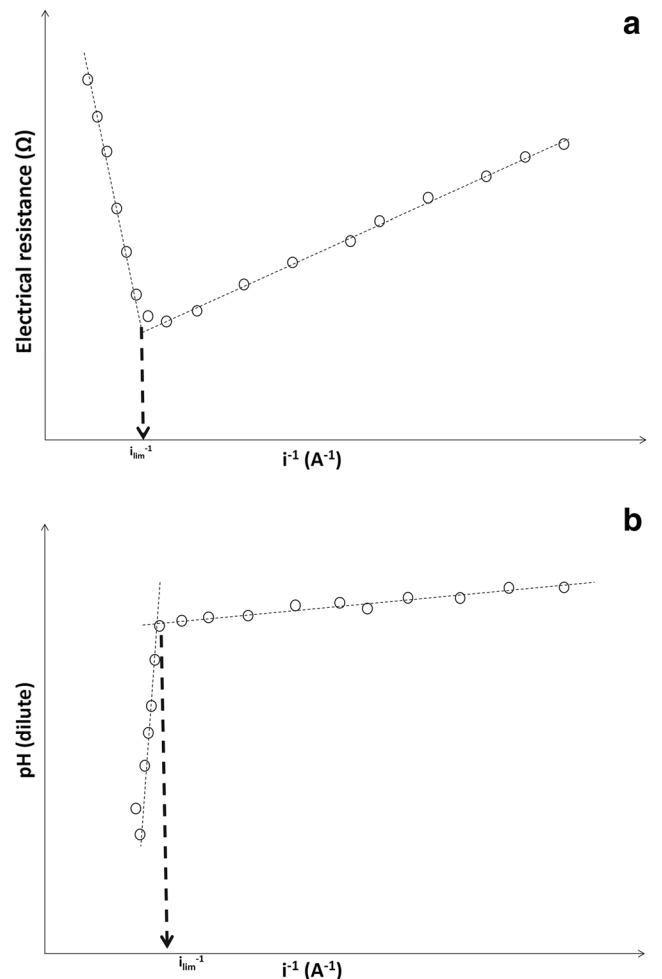


**Fig. 5** Experimental determination of  $i_{lim}$  by the Cowan–Brown method

been determined using a Metrohm pH meter model 744 (Metrohm AG, Herisau, Switzerland).

In order to remove any deposits, cleaning solutions of 0.1 M HCl, 0.1 M NaOH, and distilled water have been circulated through the ED cell for 30 min each at the end of experiment.

Usually, the limiting current depends on membrane and solution properties as well as on the electro dialysis stack construction and various operational parameters [30].

### Experimental design and statistical analysis

Experimental BBD with three numeric factors on three levels has been used. The design consists of 17 experimental runs with five replicates at the central point.

Parameters have been normalized as coded variables, so they can affect the response more evenly and the units of the parameters are irrelevant [39]. Variables have been coded according to the following equation:

$$X = \frac{(X_i - X_0)}{\Delta X} \quad (3)$$

where  $X$  is the coded value,  $X_i$  is the corresponding actual value,  $X_0$  is the actual value in the center of domain, and  $\Delta X$  is the increment of  $X$  corresponding to a variation of 1 unit of  $X$ . The natural and coded values of independent variables are presented in Table 2.

It is assumed that the independent variables are continuous and controllable by experiments with negligible errors. It is mandatory to find an appropriate approximation for the true functional relationship between independent variables and the response surface [40].

Second-order polynomial model (Eq. 4) is generally able to describe relationship between the responses and the independent variables and is usually considered as a full model in RSM.

$$Y = \beta_0 + \sum_{i=1}^2 \beta_i X_i + \sum_{i=1}^2 \beta_{ii} X_i^2 + \sum_{i < j=1}^2 \beta_{ij} X_i X_j \quad (4)$$

where  $Y$  represents the response variable,  $X_i$  and  $X_j$  are the independent variables affecting the response, and  $\beta_i$ ,  $\beta_j$ , and

**Table 2** Experimental domain with natural and coded values of independent variables used in Box–Behnken design (BBD)

Natural and coded factors	Natural and coded levels		
Calcium concentration (mol L <sup>-1</sup> ) (A)	0.0000	0.0050	0.0100
	-1	0	+1
Sulfate concentration (mol L <sup>-1</sup> ) (B)	0.0000	0.0050	0.0100
	-1	0	+1
Bicarbonate concentration (mol L <sup>-1</sup> ) (C)	0.0000	0.0025	0.0050
	-1	0	+1

$\beta_{ij}$  are the regression coefficients for intercept, linear, quadratic, and interaction terms [41–43].

Analysis of variance (ANOVA) has been used in order to evaluate model adequacy and determine regression coefficients and statistical significance.

Statistical analysis has been performed using RSM software Design-Expert v.10 Trial (Stat-Ease, Minneapolis, MN, USA).

The results have statistically been tested at the significance level of  $p = 0.05$ . The adequacy of the model has been evaluated by the coefficient of determination ( $R^2$ ), model  $p$  value, and lack of fit testing. A mathematical model has been established to describe the influence of single process parameter and/or interaction of multiple parameters on each investigated response. 3-D response surface plots have been generated with the help of the same software and drawn by using the function of two factors, keeping the others constant.

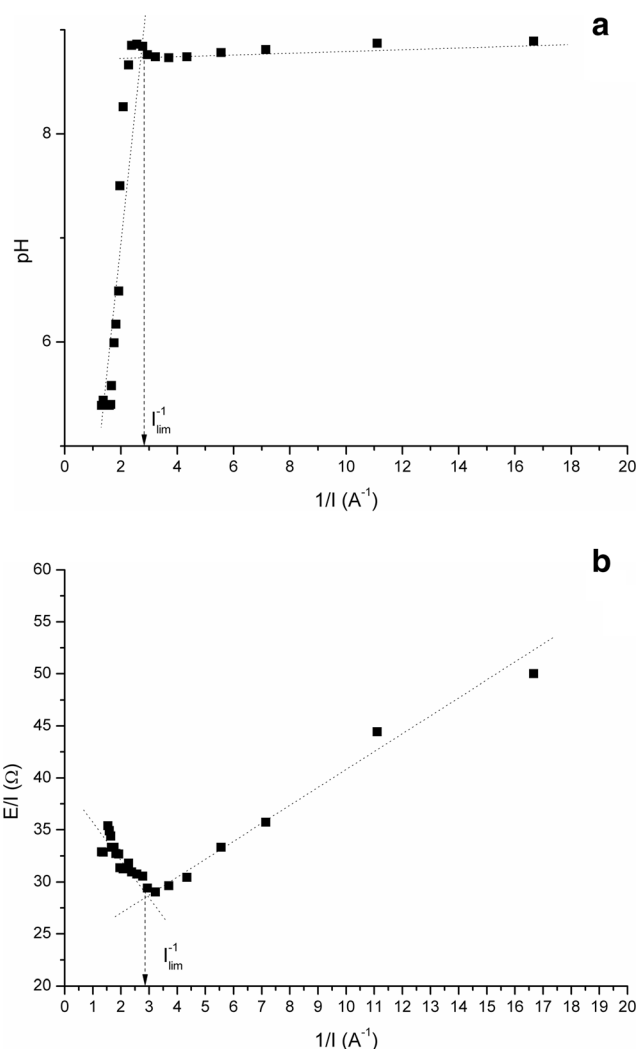


**Fig. 6** Variation of the pH of dilute (a) and the cell resistance (b) versus the reciprocal of the current: the Cowan–Brown method

## Results and discussions

### Determination of the limiting current

Figure 6 shows an example of the curves used for the determination of the limiting current from the experimental result by the Cowan–Brown method.

In the relationship between the dilute pH and the reciprocal current in Fig. 6a, the limiting current has been determined where the slope has been changed [32, 49]. In addition, the limiting current has been determined from the graph showing the cell resistance versus the reciprocal of the current (Fig. 6b).

### Application of response surface methodology

#### Model fitting

Experimental results of investigated response (limiting current density) obtained for different solutions using Box–Behnken experimental design are presented in Table 3.

Results have been fitted to a second-order polynomial model (Eq. 5), and multiple regression coefficients have been generated for the responses, using method of least square approach (MLS). The equation, in terms of coded factors, of the limiting current density is expressed as the following equation:

$$\begin{aligned} \text{LCD} = & +227.78 + 38.58 \times A - 49.68 \times B - 7.64 \\ & \times C - 8.40 \times A \times B + 3.47A \times C + 2.08 \\ & \times BC - 8.30 \times A^2 - 8.30 \times B^2 + 0.66 \times C^2 \end{aligned} \quad (5)$$

The equation in terms of coded factors (Eq. 5) can be used to make predictions about the response for given levels of each factor. By default, the high levels of the factors are coded as +1 and the low levels of the factors are coded as -1. The coded equation is useful for identifying the relative impact of the factors by comparing the factor coefficients.

The equation in terms of actual factors (Eq. 6) can be used to make predictions about the response for given levels of each factor. Here, the levels should be specified in the original units for each factor. This equation should not be used to determine the relative impact of each factor because the coefficients are scaled to accommodate the units of each factor and the intercept is not at the center of the design space.

$$\begin{aligned} \text{LCD (A m}^{-2}\text{)} = & +227.745 + 12021 \times \text{Calcium} - 5354 \\ & \times \text{Sulfate} - 5807 \times \text{Bicarbonate} - 3.358 \\ & \times 10^{+5} \times \text{Calcium} \times \text{Sulfate} + 2.776 \\ & \times 10^{+5} \times \text{Calcium} \times \text{Bicarbonate} \\ & + 1.668.10^{+5} \times \text{Sulfate} \\ & \times \text{Bicarbonate} - 3.321 \times 10^{+5} \\ & \times \text{Calcium}^2 - 3.321 \times 10^{+5} \times \text{Sulfate}^2 \\ & + 1.060 \times 10^{+5} \times \text{Bicarbonate}^2 \end{aligned} \quad (6)$$

**Table 3** Box–Behnken experimental design with natural and coded variables and experimentally obtained values of investigated response

Run	Coded variable			Natural variable			Response LCD (A m <sup>-2</sup> )
	A	B	C	Calcium (mol L <sup>-1</sup> )	Sulfate (mol L <sup>-1</sup> )	Bicarbonate (mol L <sup>-1</sup> )	
1	0	0	0	0.005	0.005	0.0025	227.78
2	0	1	-1	0.005	0.010	0.0000	172.22
3	0	0	0	0.005	0.005	0.0025	227.78
4	-1	-1	0	0.000	0.000	0.0025	213.89
5	0	0	0	0.005	0.005	0.0025	227.78
6	0	0	0	0.005	0.005	0.0025	227.78
7	0	-1	1	0.005	0.000	0.0050	263.89
8	1	1	0	0.010	0.010	0.0025	191.67
9	1	0	-1	0.010	0.005	0.0000	266.67
10	-1	1	0	0.000	0.010	0.0025	133.33
11	-1	0	1	0.000	0.005	0.0050	166.67
12	0	1	1	0.005	0.010	0.0050	166.67
13	0	-1	-1	0.005	0.000	0.0000	277.78
14	0	0	0	0.005	0.005	0.0025	227.78
15	1	0	1	0.010	0.005	0.0050	252.78
16	-1	0	-1	0.000	0.005	0.0000	194.44
17	1	-1	0	0.010	0.000	0.0025	305.81

To evaluate the model, an ANOVA was applied and the results of the analysis of the model are presented in Table 4.

The statistical significance of the model is assigned according to *F* value. The “model *F* value” of 329.70 implies that the model is highly significant.

There is only a 0.01% chance that a “model *F* value” with this magnitude could occur due to noise. A very low probability value (*p* value < 0.0001) implies that the model is strongly significant over the 95% confidence interval (i.e., *p* values less than 0.05 indicate significance).

The nonsignificance of lack-of-fit is favorable and it specifies the high predictability of the model. The “lack of fit *F* value” of 78.04 implies the lack of fit is not significant relative to the pure error.

Predicted versus actual plot of LCD is shown in Fig. 7.

The values predicted by the model (from Eq. 5) and the results obtained by the experiments are distributed uniformly around a 45° line.

The coefficient of determination, which is defined as the ratio of the explained variation to total variation, is very close to unity (0.9976).

**Table 4** Analysis of variance (ANOVA) for the fitted model

Source	Sum of squares	<i>df</i>	Mean square	<i>F</i> value	<i>p</i> value Prob > <i>F</i>
Model	33,080.16	9	3675.57	329.70	<0.0001 Significant
Residual	78.04	7	11.15		
Lack of fit	78.04	3	26.01		
Pure error	0.000	4	0.000		
Total	33,158.20	16			
<i>R</i> -squared	0.9976		Std. Dev.	3.34	
Adj <i>R</i> -squared	0.9946		Adeq precision	68.931	
Pred <i>R</i> -squared	0.9623		CV %	1.52	

This provides further support of a precise correlation between the actual and the predicted values.

The high value of the adjusted determination coefficient ( $R^2$  adj = 0.9946) indicates that the second-order polynomial is very capable of representing the process under the given experimental domain.

The adequate precision (AP) is defined by the measurement range of the predicted response relative to its associated error which means the signal-to-noise ratio. A ratio greater than 4 is desirable. The obtained value for AP (68.931) indicates an adequate signal. This proves that the model can be used to navigate the design space, and as the final clue in this section, it should be noted that the low value for coefficient of variation (CV% = 1.52) demonstrates dependability and reproducibility of the model.

The significance of the parameter coefficients and the associated standard error of each term in Eq. 5 are presented in Table 5.

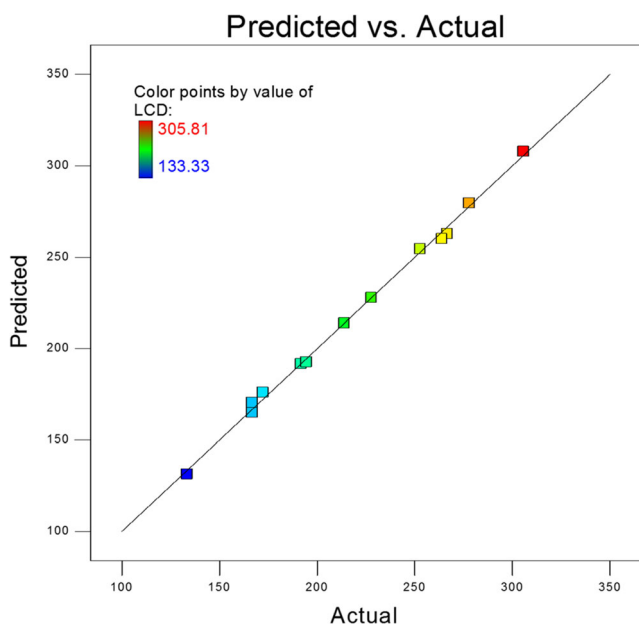


**Fig. 7** Predicted versus actual plot of LCD

Values of “Prob > *F*” less than 0.0500 indicate model terms are significant. In this case, *A*, *B*, *C*, *AB*,  $A^2$ , and  $B^2$  are significant model terms. Values greater than 0.1000 indicate the model terms are not significant. If there are many insignificant model terms (not counting those required to support hierarchy), model reduction may improve your model.

The ANOVA results reveal that the significance of studied parameters on limiting current density is (the most to the least significant) sulfate concentration > calcium concentration > bicarbonate concentration.

The highest *F* value (1771.47) and the lowest *p* value (<0.0001) are assigned to the sulfate concentration among other variables.

This result indicates that the concentration of sulfate in the treated solution is the most important parameter affecting the limiting current density of an electro dialysis process under the current circumstances.

The ANOVA results of Table 5 suggest that only the binary interaction *AB* is significant. The *C* factor has no significant interactions with the two other parameters.

**Table 5** ANOVA results for the coefficients of the fitted second-order polynomial model

Source	Sum of squares	<i>df</i>	Mean square	<i>F</i> value	<i>p</i> value Prob > <i>F</i>
<i>A</i> —calcium	11,904.25	1	11,904.25	1067.81	<0.0001
<i>B</i> —sulfate	19,748.79	1	19,748.79	1771.47	<0.0001
<i>C</i> —bicarbonate	466.65	1	466.65	41.86	0.0003
<i>AB</i>	281.90	1	281.90	25.29	0.0015
<i>AC</i>	48.16	1	48.16	4.32	0.0763
<i>BC</i>	17.39	1	17.39	1.56	0.2518
$A^2$	290.24	1	290.24	26.03	0.0014
$B^2$	290.24	1	290.24	26.03	0.0014
$C^2$	1.85	1	1.85	0.17	0.6961



The effects of the parameters on the limiting current density

A perturbation plot shows the comparison among the effects of all the factors at a particular point in the design space. The perturbation plot for the limiting current density of an electro-dialysis process is shown in Fig. 8.

LCD has been plotted by means of changing only one factor over its range while keeping other factors constant. The plot gives the effects of all factors at the central point (calcium concentration = 0.005 M, sulfate concentration = 0.005 M, bicarbonate concentration = 0.0025 M).

The curvature and the slope of A, B line indicate that the response is sensitive to these factors. However, the low value of C line slope confirm that the LCD is not really depending on this parameter. It can be observed from Eq. 5 and the perturbation plot that the limiting current density increases approximately linearly with calcium concentration and decreases more by increasing the sulfate concentration of treated solution in the investigated design space.

In addition to the ANOVA results of Table 5, the elliptical shape of the contour plots demonstrates the significance of the investigated interactions on the response. If the contour lines were parallel with either of the axes, no interaction would exist between the two variables. As seen in Fig. 9, only interaction AB is significant.

In order to have a complete understanding of the effects of the solution composition of a treated solution on the limiting current density of an electro-dialysis process, along with the two-dimensional contours, three-dimensional response surface plots are essential.

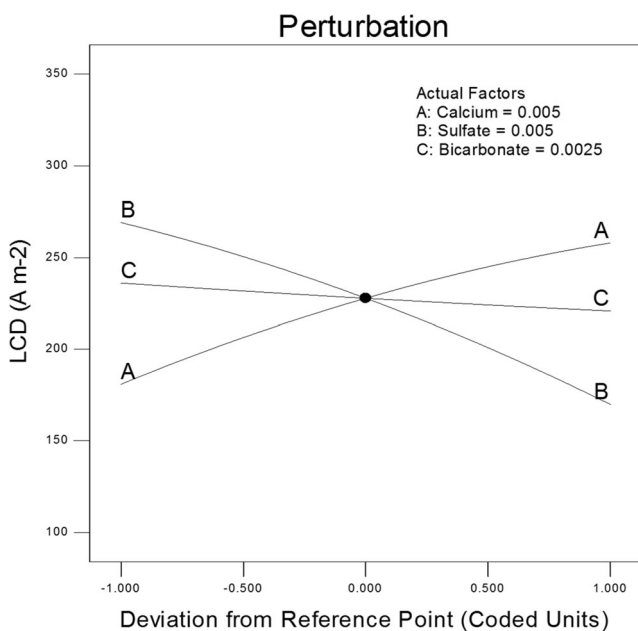


Fig. 8 The perturbation plot for the LCD (a calcium concentration, b sulfate concentration, c bicarbonate concentration)

In each plot, two factors are changed while one is kept constant at the central point. Figures 9a and 10a show the simultaneous influence of calcium and sulfate bicarbonate concentration on LCD.

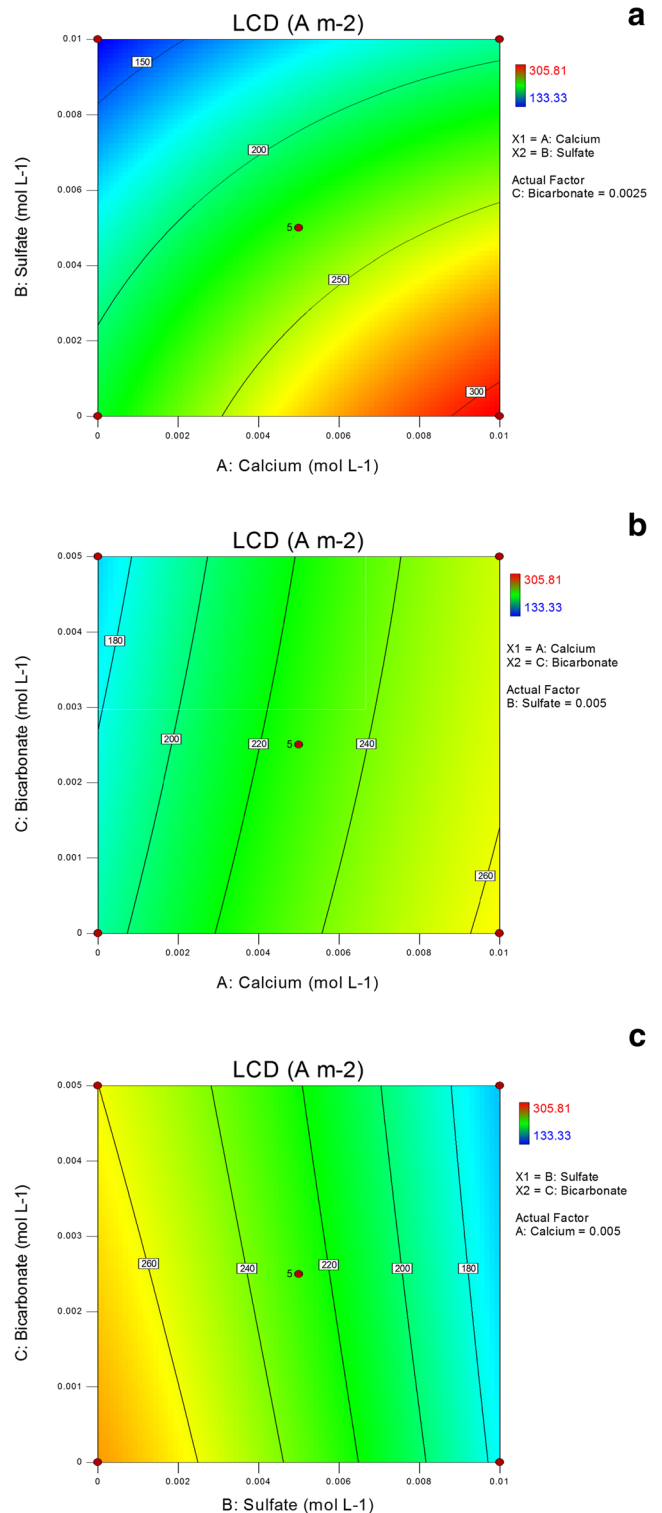
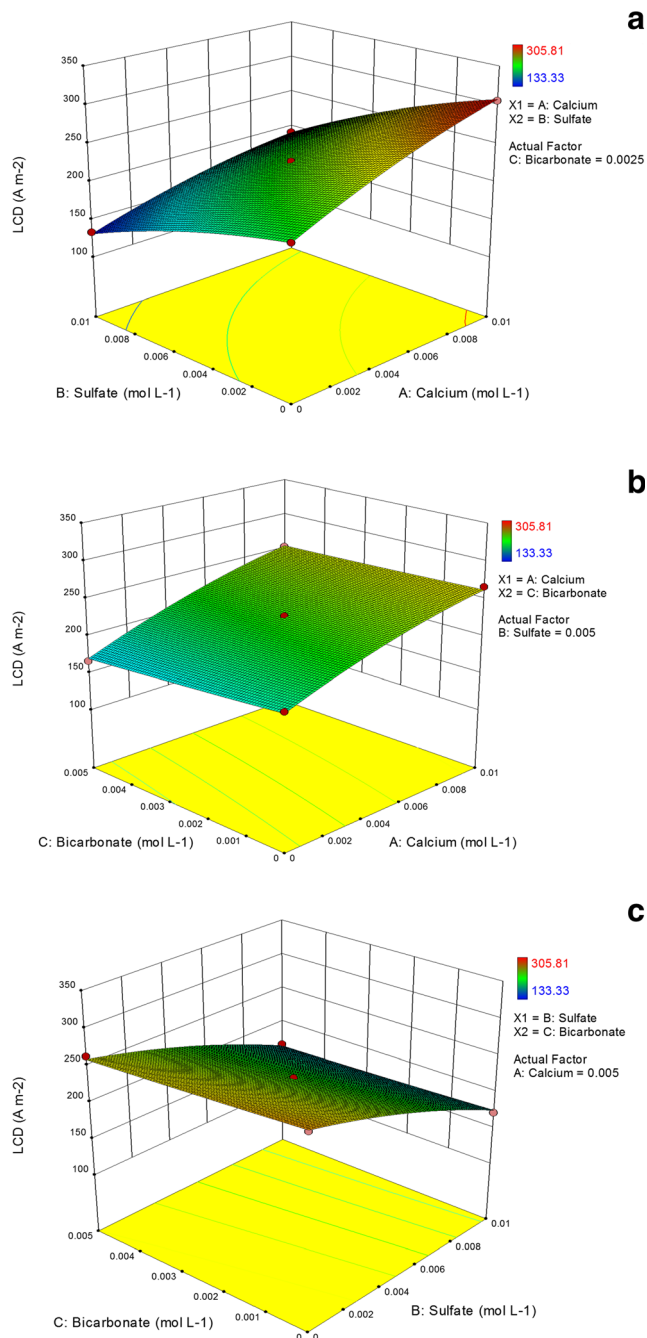


Fig. 9 The contour plots showing simultaneous interaction between a calcium and sulfate concentration, b calcium and bicarbonate concentration, and c sulfate and bicarbonate concentration on LCD



**Fig. 10** The response surface plots showing simultaneous interaction between **a** calcium and sulfate concentration, **b** calcium and bicarbonate concentration, and **c** sulfate and bicarbonate concentration on LCD

At a constant bicarbonate concentration, higher LCD have been obtained for highest calcium concentration and lowest sulfate concentration. The increase in the calcium concentration up to 0.004 M for solution containing a concentration of sulfate under 0.002 M leads to an increase in LCD more than  $260 \text{ A m}^{-2}$ .

As shown in Figs. 9c and 10c, the study of the interaction between bicarbonate and sulfate concentration on the LCD

shows the same results. At fixed calcium concentration, LCD decreases by increasing the sulfate concentration.

Figures 9b and 10b show the interaction between calcium and bicarbonate concentration. As can be seen, the two factors follow similar trends, an increase in the calcium dosage from 0.001 to 0.01 M and the bicarbonate concentration from 0 to 0.005 M increase the LCD.

In conclusion, the limiting density depends on the composition of the solution. The sulfate concentration seems to be the most influencing parameter. The existence of these anions in the solution can strongly reduce the value of the limiting current density and therefore the efficiency of the electro dialysis process is affected.

This can be interpreted by the different motilities of various ions present at the membrane/solution interface and precisely at the diffusion boundary layer of the membrane surface.

These results can confirm our finding in a previous study [27]. Effectively, previous work showed that the presence of divalent anions has an effect on the desalination process. We found that the presence of sulfate ions affects the demineralization rate. Indeed, the addition of these anions decreases the process efficiency. The effect of sulfate ions is clearly noted on the calcium ionic transfer. Certainly, the presence of these anions largely reduces the transfer of calcium ions during the desalination process at very low fluxes. This result can be interpreted by the fact that in the presence of bivalent anions, Calcium ions are retained in the dilute. Apparently, the mobility of these cations decreases. A mutual interaction between the oppositely charged ions can take place. The efficiency decreases more and more by increasing the molar fraction of the  $\text{SO}_4^{2-}$  ions in the solution. This phenomenon can reduce strongly the concentration of these ions at the diffusion boundary layer of the membrane surface facing the dilute cell and a polarization phenomenon can occur.

On the other side of membrane, at the surface facing the concentrate compartment, the concentration of charged species increases. In fact, due to the dipolar interactions between sulfate anions and cations present at this region and due to high transfer of cations through the ion exchange membrane, the probability of accumulation of salt can increase and the concentration polarization can be reached at low applied current.

As a consequence, lower LCD can be obtained for solution containing high levels of sulfate.

The bicarbonate anions can also affect the LCD, but their influence is not so important compared to the effect of sulfate ions.

The limiting current density depends too on the presence of bivalent cations in the solution. The higher the calcium concentrations are, the higher the LCD value is. This is due to the fact that the quantities of charged species in the solution are sufficient to assure the transport of current in all compartments and cell resistivity still relatively

low. These results also confirm our findings in a previous work [44]. For solutions containing only NaCl salt, highest LCD have been obtained for higher initial salt concentrations (more than 0.05 M).

As mentioned before, better desalination efficiency will be obtained by increasing the applied current [27, 31, 33, 45].

## Conclusions

BBD combined with RSM has been successfully applied to develop an explicit model to estimate the LCD as a function of the composition of solution to be treated by electro dialysis.

Due to satisfactory parameters of descriptive statistics ( $R^2$  and CV %) and ANOVA for the model and lack of fit testing, it could be concluded that second-order polynomial model provided adequate mathematical description of limiting current density under the given experimental domain.

For further investigations, it would be worth studying and examining the model at a higher range of concentration, for other types of monovalent and divalent ions, and in larger scales.

According to ANOVA results, it has been shown that the limiting density depends on the composition of the solution. The sulfate concentration seems to be the most influencing parameter. The existence of these anions in the solution can reduce strongly the value of the limiting current density and consequently the efficiency of the electro dialysis process is affected.

**Acknowledgements** The authors are sincerely grateful to Dr. Chaouki M'kaddem, Senior Teacher of English at the Ministry of Education of Tunisia, for proofreading and editing our manuscript.

## References

1. Ghyselbrecht K, Huygebaert M, Van der Bruggen B, Ballet R, Meesschaert B, Pinoy L (2013) Desalination of an industrial saline water with conventional and bipolar membrane electro dialysis. *Desalination* 318:9–18. doi:10.1016/j.desal.2013.03.020
2. Ghyselbrecht K, Silva A, Van der Bruggen B, Boussu K, Meesschaert B, Pinoy L (2014) Desalination feasibility study of an industrial NaCl stream by bipolar membrane electro dialysis. *J Environ Manag* 140:69–75
3. Moon S-H, Yun S-H (2014) Process integration of electro dialysis for a cleaner environment. *Current Opinion in Chemical Engineering* 4:25–31
4. Xu T, Huang C (2008) Electro dialysis-based separation technologies: a critical review. *AIChE J* 54(12):3147–3159. doi:10.1002/aic.11643
5. Banasiak LJ, Schäfer AI (2009) Removal of boron, fluoride and nitrate by electro dialysis in the presence of organic matter. *J Membr Sci* 334(1–2):101–109
6. Dementzis K (2010) Removal of nickel from electroplating rinse waters using electrostatic shielding electro dialysis/electrodeionization. *J Hazard Mater* 173(1–3):647–652. doi:10.1016/j.jhazmat.2009.08.133
7. Karimi L, Ghassemi A (2016) An empirical/theoretical model with dimensionless numbers to predict the performance of electro dialysis systems on the basis of operating conditions. *Water Res* 98:270–279. doi:10.1016/j.watres.2016.04.014
8. Káňavová N, Machuča L, Tvrzňik D (2014) Determination of limiting current density for different electro dialysis modules. *Chem Pap* 68(3):324–329
9. Krol JJ, Wessling M, Strathmann H (1999) Concentration polarization with monopolar ion exchange membranes: current–voltage curves and water dissociation. *J Membr Sci* 162(1–2):145–154. doi:10.1016/S0376-7388(99)00133-7
10. Meng H, Deng D, Chen S, Zhang G (2005) A new method to determine the optimal operating current ( $i_{lim}$ ) in the electro dialysis process. *Desalination* 181(1):101–108
11. Geraldes V, Afonso MD (2010) Limiting current density in the electro dialysis of multi-ionic solutions. *J Membr Sci* 360(1–2):499–508. doi:10.1016/j.memsci.2010.05.054
12. Tanaka Y (2005) Limiting current density of an ion-exchange membrane and of an electro dialyzer. *J Membr Sci* 266(1–2):6–17. doi:10.1016/j.memsci.2005.05.005
13. Tanaka Y (2006) Irreversible thermodynamics and overall mass transport in ion-exchange membrane electro dialysis. *J Membr Sci* 281(1–2):517–531. doi:10.1016/j.memsci.2006.04.022
14. Tanaka Y (2012) Ion-exchange membrane electro dialysis program and its application to multi-stage continuous saline water desalination. *Desalination* 301:10–25. doi:10.1016/j.desal.2012.06.007
15. Nakayama A, Sano Y, Bai X, Tado K (2017) A boundary layer analysis for determination of the limiting current density in an electro dialysis desalination. *Desalination* 404:41–49. doi:10.1016/j.desal.2016.10.013
16. Wang Y, Huang C, Xu T (2010) Optimization of electro dialysis with bipolar membranes by using response surface methodology. *J Membr Sci* 362(1–2):249–254. doi:10.1016/j.memsci.2010.06.049
17. Zazouli MA, Dianati Tilaki RA, Safarpour M (2014) Modeling nitrate removal by nano-scaled zero-valent iron using response surface methodology. *Health Scope* 3(3):e15728
18. Fouladitajar A, Ashtiani FZ, Dabir B, Rezaei H, Valizadeh B (2014) Response surface methodology for the modeling and optimization of oil-in-water emulsion separation using gas sparging assisted microfiltration. *Environmental Science and Pollution Research*:1–17
19. Mourabet M, El Rhilassi A, El Boujaady H, Bennani-Ziatni M, Taitai A (2014) Use of response surface methodology for optimization of fluoride adsorption in an aqueous solution by Brushite. *Arab J Chem*. doi:10.1016/j.arabc.2013.12.028
20. Mourabet M, El Rhilassi A, El Boujaady H, Bennani-Ziatni M, El Hamri R, Taitai A (2012) Removal of fluoride from aqueous solution by adsorption on Apatitic tricalcium phosphate using Box–Behnken design and desirability function. *Appl Surf Sci* 258(10):4402–4410. doi:10.1016/j.apsusc.2011.12.125
21. Boubakri A, Hafiane A, Bouguecha SAT (2014) Application of response surface methodology for modeling and optimization of membrane distillation desalination process. *J Ind Eng Chem* 20(5):3163–3169. doi:10.1016/j.jiec.2013.11.060
22. Boubakri A, Bouchrit R, Hafiane A, Bouguecha SA-T (2014) Fluoride removal from aqueous solution by direct contact membrane distillation: theoretical and experimental studies. *Environ Sci Pollut Res*:1–9
23. Ferreira SLC, Bruns RE, Ferreira HS, Matos GD, David JM, Brandão GC, da Silva EGP, Portugal LA, dos Reis PS, Souza AS, dos Santos WNL (2007) Box–Behnken design: an alternative for the optimization of analytical methods. *Anal Chim Acta* 597(2):179–186. doi:10.1016/j.aca.2007.07.011

- 24 Aslan N, Cebeci Y (2007) Application of Box–Behnken design and response surface methodology for modeling of some Turkish coals. *Fuel* 86(1–2):90–97. doi:10.1016/j.fuel.2006.06.010
- 25 Isgoren M, Gengec E, Veli S (2016) Evaluation of wet air oxidation variables for removal of organophosphorus pesticide malathion using Box–Behnken design. *Water Sci Technol*. doi:10.2166/wst.2016.479
- 26 Sahoo C, Gupta AK (2012) Optimization of photocatalytic degradation of methyl blue using silver ion doped titanium dioxide by combination of experimental design and response surface approach. *J Hazard Mater* 215–216:302–310. doi:10.1016/j.jhazmat.2012.02.072
- 27 Ben Sik Ali M, Hafiane A, Dhahbi M, Hamrouni B (2014) Desalination of brackish water by electrodialysis: effects of operational parameters and water composition on process efficiency. In: Daniels JA (ed) *Advances in environmental research*. Volume 32. *Advances in environmental research*. Nova Science Publishers, New York, p 372
- 28 Alvarado L, Chen A (2014) Electrodeionization: principles, strategies and applications. *Electrochim Acta* 132:583–597. doi:10.1016/j.electacta.2014.03.165
- 29 Zerdoumi R, Oulmi K, Benslimane S (2014) Electrochemical characterization of the CMX cation exchange membrane in buffered solutions: effect on concentration polarization and counterions transport properties. *Desalination* 340:42–48. doi:10.1016/j.desal.2014.02.014
- 30 Doyen A, Roblet C, L'Archevêque-Gaudet A, Bazinet L (2014) Mathematical sigmoid-model approach for the determination of limiting and over-limiting current density values. *J Membr Sci* 452:453–459
- 31 Ben Sik Ali M, Mnif A, Hamrouni B, Dhahbi M (2010) Electrodialytic desalination of brackish water: effect of process parameters and water characteristics. *Ionics* 16(7):621–629. doi:10.1007/s11581-010-0441-2
- 32 Baker RW (2004) *Membrane technology and applications*, 2nd edn. John Wiley & Sons, Ltd., England
- 33 Noble RD, Stern SA (1995) *Membrane separations technologies principles and applications*, Membrane science and technology series, vol 2. Elsevier Science B.V., Amsterdam
- 34 Strathmann H (2010) Electrodialysis, a mature technology with a multitude of new applications. *Desalination* 264(3):268–288. doi:10.1016/j.desal.2010.04.069
- 35 Nikonenko VV, Kovalenko AV, Urtenov MK, Pismenskaya ND, Han J, Sizat P, Pourcelly G (2014) Desalination at overlimiting currents: state-of-the-art and perspectives. *Desalination* 342:85–106
- 36 Tanaka Y (2002) Current density distribution, limiting current density and saturation current density in an ion-exchange membrane electrolyszer. *J Membr Sci* 210(1):65–75
- 37 Lee HJ, Sarfert F, Strathmann H, Moon SH (2002) Designing of an electrodialysis desalination plant. *Desalination* 142(3):267–286
- 38 Długolecki P, Anet B, Metz SJ, Nijmeijer K, Wessling M (2010) Transport limitations in ion exchange membranes at low salt concentrations. *J Membr Sci* 346(1):163–171. doi:10.1016/j.memsci.2009.09.033
- 39 Baş D, Boyacı İH (2007) Modeling and optimization I: usability of response surface methodology. *J Food Eng* 78(3):836–845. doi:10.1016/j.jfoodeng.2005.11.024
- 40 Kwak J-S (2005) Application of Taguchi and response surface methodologies for geometric error in surface grinding process. *Int J Mach Tools Manuf* 45(3):327–334. doi:10.1016/j.ijmachtools.2004.08.007
- 41 Zuorro A, Fidaleo M, Lavecchia R (2013) Response surface methodology (RSM) analysis of photodegradation of sulfonated diazo dye Reactive Green 19 by UV/H<sub>2</sub>O<sub>2</sub> process. *J Environ Manag* 127:28–35. doi:10.1016/j.jenvman.2013.04.023
- 42 Šumić Z, Vakula A, Tepić A, Čakarević J, Vitas J, Pavlič B (2016) Modeling and optimization of red currants vacuum drying process by response surface methodology (RSM). *Food Chem* 203:465–475. doi:10.1016/j.foodchem.2016.02.109
- 43 Sohrabi S, Akhlaghian F (2016) Modeling and optimization of phenol degradation over copper-doped titanium dioxide photocatalyst using response surface methodology. *Process Saf Environ Prot* 99:120–128. doi:10.1016/j.psep.2015.10.016
- 44 Ben Sik Ali M, Hamrouni B (2016) Development of a predictive model of the limiting current density of an electrodialysis process using response surface methodology. *Membrane Water Treatment* 7(2):127–141. doi:10.12989/mwt.2016.7.2.127
- 45 Strathmann H (2004) *Ion-exchange membranes separation processes*, vol 9. Membrane Science and Technology Series. Elsevier B.V, Amsterdam
- 46 Cavazzuti M (2012) *Optimization methods: from theory to design scientific and technological aspects in mechanics*. Springer Science & Business Media
- 47 Wang Y, Huang C, Xu T (2010) Optimization of electrodialysis with bipolar membranes by using response surface methodology. *J Membr Sci* 362(1–2):249–254
- 48 Ben Sik Ali M, Mnif A, Hamrouni B, Dhahbi M, (2010) Electrodialytic desalination of brackish water: effect of process parameters and water characteristics. *Ionics* 16(7):621–629
- 49 Lee H-J, Strathmann H, Moon S-H (2006) Determination of the limiting current density in electrodialysis desalination as an empirical function of linear velocity. *Desalination* 190(1–3):43–50